Electrical machines fault detection

Lucia FROSINI

Department of Electrical, Computer and Biomedical Engineering,
University of Pavia
Pavia, Italy
E-mail: lucia@unipv.it

What is the diagnostics?

The diagnostics is a procedure of "translation" of the information arising from the measurement of parameters related to a machine (or a system) in information regarding the effective or incipient faults of the machine itself.

In other words, the diagnostics is the complex of the activities of analysis and synthesis which - by using the acquisition of certain physical quantities, characteristic of the monitored machine - allows to draw significant information on the condition of the machine and on its trend during the time, for the evaluation of its reliability in short and long term.

The targets of the diagnostics are:

- detection,
- isolation,
- identification.

} of the fault

The hypothesis test

The general problem of the diagnostics is to detect if a specific fault is present (or not) on the basis of the available information, preferably without an intrusive inspection of the machine.

This problem can be described with a statistical approach as a problem of hypothesis test:

- null hypothesis H_0: the fault is present;
- alternative hypothesis H_1: the fault is not present.

The hypothesis test is subject to two types of error:

- type I error happens when the null hypothesis H_0 is true and you reject it, e.g. when, on the basis of the available information, you decide that fault is not present, but actually it is. Therefore, the machine is not stopped and repaired before the effective manifestation of the failure, with possible catastrophic consequences.

The steps of the diagnostics

- type II error happens when the null hypothesis is false and you fail to reject it, e.g. when, on the basis of the available information, you decide that fault is present, but actually it is not present. Therefore, the machine is stopped and repaired in vain, with useless economic costs.

→ Diagnostics is not an exact science!

A diagnostic program develops according to the following steps:

- data acquisition,
- data processing,
- decision-making.

The methods employed for the acquisition and elaboration of the data and for the choice of the threshold which separates the faulty condition from the healthy condition of a component can heavily influence the chance to incur an error during the phase of the decision making.

The objects of the diagnostics

If the objects of our diagnostics are the rotating electrical machines, it is important to note that the operation of these machines cannot be considered separately from:

- the operation of the mechanical machines connected along its axis line, e.g. turbines or other prime motors for the electrical generators, pumps or fans or other loads for the electrical motors;
- the type of the mechanical coupling, e.g. joints, gears, belts, etc.;
- the possible control system (inverter, etc.).

All these mechanical and electronic systems can:

- induce faults in the electrical machine,
- arouse changes in the parameters of the electrical machine, even in absence of fault;
- experience faults induced by the electrical machine.

The main parts of the induction motor

In the following we will consider, as objects of our diagnostics, only the induction motors and in particular those with cage rotor, since they are more widespread with respect to those with wound rotor.

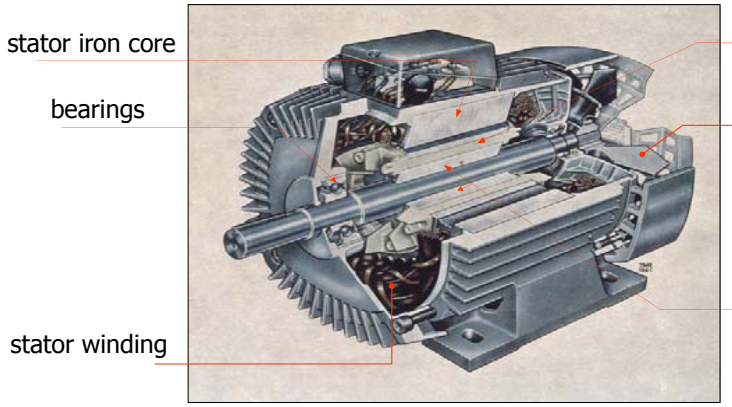

Where the faults can happen in the motors?

In the literature, only two extensive (and quite old) surveys on the faults in electrical motors are present, one dated 1985 and the other one 1995: since the latter is limited to the petrochemical industry, normally the authors refer to the results reported in the first survey, developed by the Electric Power Research Institute (EPRI):

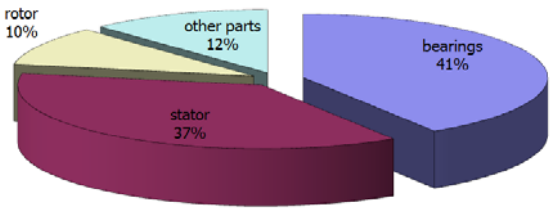

Note that the frequency of occurrence of these faults depends heavily on the specific application of the machine.

Possible indicators of fault

The diagnostics and the condition monitoring require the measurement and the analysis of some signals that contain characteristic information (symptoms) about the process of wear, malfunctions or incipient faults.

The following factors should be considered in the selection of the more appropriate diagnostic techniques:

1) The sensor should be (possibly) non-invasive;
2) The sensor and the measurement system must be reliable;
3) The diagnosis must be reliable;
4) The severity of the problem should be quantified;
5) Ideally, you should have an evaluation of the remaining life time;
6) Ideally, the information obtained from the sensor should provide an indication of the "root causes" which produced the fault.

Possible indicators of fault

In many cases, it is possible to meet the criteria from 1) to 4), whereas those from 5) to 6) are extremely difficult to achieve.

In an electrical machine, different aspects (electrical, magnetic, mechanical, fluid dynamics, thermal) interact in a complex manner, as shown in the figure:

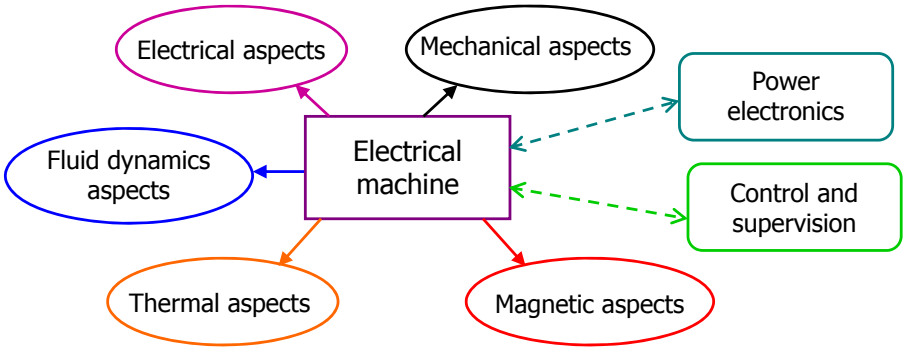

Possible indicators of fault

Various parameters belonging to these different fields can be suitable as potential fault indicators:

Electromagnetic:
- current, voltage → **Motor Current Signature Analysis (MCSA)**
- partial discharges
- magnetic fluxes (internal and external)

Mechanical:
- vibrations (displacement, speed, acceleration)
- noise (acoustic emission)
- angular speed
- force, torque

Other (thermal, chemical):
- temperature
- analysis of oil and gas (for transformers)

Possible indicators of fault

If present, the control and supervision system governing the overall installation and the power electronics specializing in translating the commands in energy signals supplied to the machine can be considered together as an important part in the scheme of diagnostics and condition monitoring.

Further possible indicators of fault are:

- The measurement of the efficiency, which requires the measurement of both the input and the output power (therefore both electrical and mechanical parameters) in case of rotating electrical machine.
- The visual analysis of different parts of the machine, during the revisions involving their dismantling: this analysis is based on objective parameters, but also on the experience of the technical staff.

MCSA to detect induction motor faults

Many research papers have been written about this issue in the last decades.

The possible faults which can be detected by means of MCSA are:

1) Broken rotor bars
2) Rotor eccentricities

- slowly progressive faults
- primary effect on airgap flux and therefore on stator current
- well known and established methodology, from many years

3) Stator short circuits →
- quickly progressive fault
- primary effect on airgap flux and therefore on stator current
- well known theory, but still not applied in real cases

4) Bearing faults →
- slowly progressive fault
- secondary (and often weak) effect on airgap flux and therefore on stator current
- well known theory (but not valid for any type of bearing fault), still not applied in real cases

Broken rotor bars

Broken rotor bars can be a serious problem, especially for large induction motors with arduous duty cycles.

Although broken rotor bars do not initially cause an induction motor to fail, there can be serious secondary effects: the fault mechanism can result in broken parts of the bar hitting the end winding or the stator core of a high-voltage motor at high speed. This can cause a serious mechanical damage to the insulation and a consequential winding failure may follow, resulting in a costly repair and lost production.

Broken rotor bars or end rings can be caused by:

- Direct-on-line starting duty cycles for which the rotor cage winding was not designed to withstand;
- Pulsating mechanical loads;
- Imperfections in the manufacturing process of the rotor cage.

W.T. Thomson, R.J. Gilmore, "Motor current signature analysis to detect faults in induction motor drives – Fundamentals, data interpretation, and industrial case histories", in *Proc. Turbomachinery Symposium*, pp. 145-156, Houston (Texas), USA, 2003.

Types of rotor

Induction machines can be equipped with the following types of rotor:

- wound rotor, with a three-phase winding consisting of copper wires or strips and three short-circuit rings.
- squirrel cage rotor, with a multi-phase winding consisting of bars and two frontal short-circuit rings. The cage rotor can be die-cast or fabricated (with the bars inserted in the slots and welded to the frontal rings). In the first case, the bars are almost always made of aluminum (but they can be made of copper or copper alloys), whereas in the second case they are almost always made of copper.

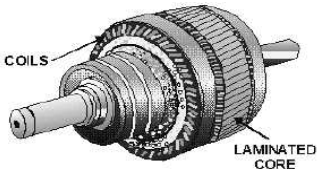

WOUND ROTOR

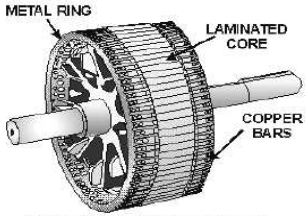

SQUIRREL-CAGE ROTOR

Die-cast cage rotor

The die-cast cage rotor is used in low-power induction motors (<50÷100 kW).

The whole cage is formed in a single piece by pouring molten metal (usually aluminum) into a mold.

The bars are generally skewed with respect to the stator slots.

Die-cast cage rotor

In recent years, the manufacturing technique of die-cast copper cage rotors is spreading, in order to improve the motor efficiency.

The manufacturing process of this type of rotor, compared to the die-cast aluminium cage, presents higher energetic and economic costs and it is technically more complex.

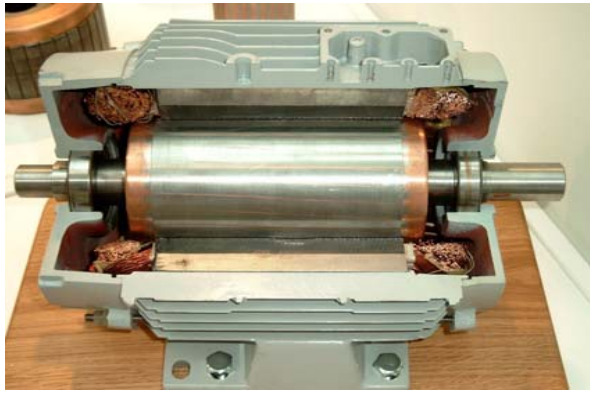

Fabricated cage rotor

For higher power induction motors (>50÷100 kW), generally (but not always) supplied at high voltage (>700 V), the rotor consists of copper bars that are inserted into the slots and welded to the frontal short circuit rings.

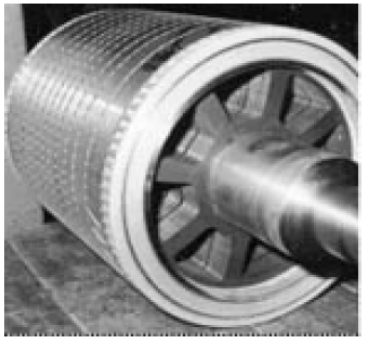

900 kW, 6000 V, 8 poles

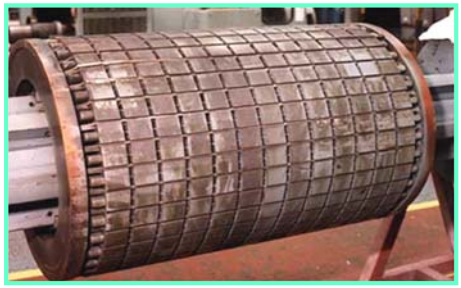

2800 kW, 6600 V, 2 poles

Fabricated cage rotor

Other examples of fabricated cage rotors:

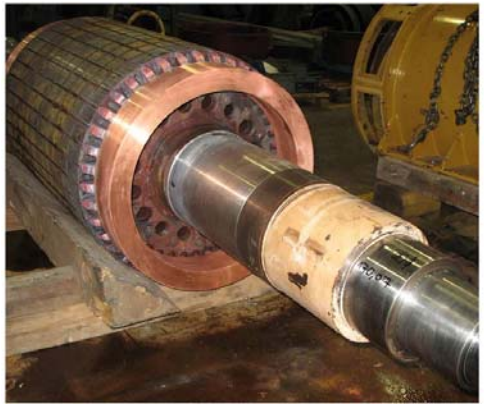

Fabricated cage rotor for a 3 MW motor, 6 kV, 2 poles

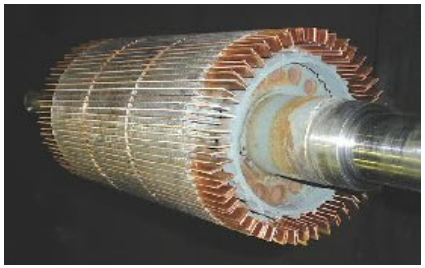

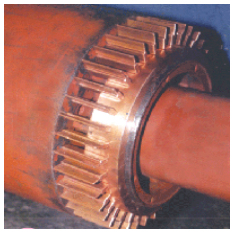

300 kW, 3300 V

Fabricated cage rotor

For these rotors, the most likely failure is due to the breakage of a bar or a fracture near the joint between bars and rings.

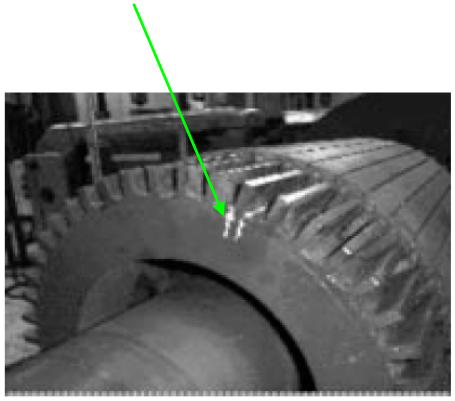

900 kW, 6 kV, 8 poles

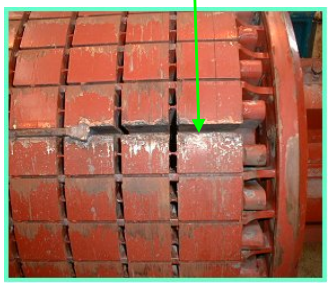

3100 kW, 11 kV, 2 poles

Fabricated cage rotor

Other examples of rotors with broken bars:

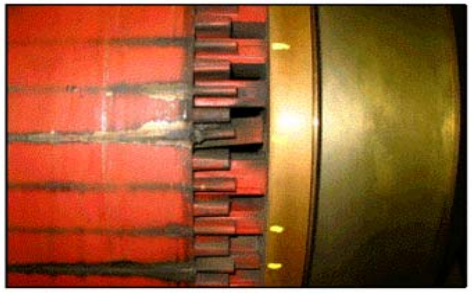

Ex.: 2600 kW, 4160 V, 2 poles

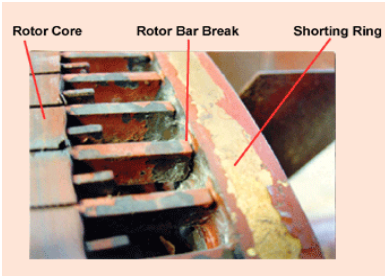

If the failure is detected before the complete breakdown of the motor:
Motor repair cost: $ 60,000 (repair) + $ 30,000 (planned plant shutdown).
Otherwise: motor replacement cost: $ 170,000 (new motor) + $ 200,000 (unscheduled plant shutdown).

http://pdma.com/pdfs/cs/Case_Studies_in_Online_and_Offline_Motor_Analysis.pdf

Rotor bar breaking

This failure is generally caused by thermal stresses and frequent start-ups.

This deterioration is slowly progressive, therefore a diagnostic tool can be effective in preventing it!

The start-up is a critical phase for the cage: the high temperature produced by the high currents causes expansion of the bars, favoring the possible occurrence of fractures or detachments at the point of contact between bars and rings (due to mechanical fatigue, welding failure, etc.).

The consequent increase of impedance in the bar subject to the failure results in a redistribution of the currents in the healthy bars, arousing an imbalance of the magnetic flux produced by the rotor, which in turn causes an imbalance in the stator currents.

Rotor bar breaking

This imbalance produces a resultant backward rotating field, with a consequent increase of the currents in both windings (remarkable on the rotor, lower on the stator) and an increase of their temperatures.

The redistribution of the currents in the healthy bars, associated with the temperature increase, results in increased mechanical and thermal stresses on the adjacent bars to the broken one.

This causes the propagation of the failure.

This is usually a chain phenomenon, as the first broken bar causes more stress on the adjacent bars, which therefore deteriorates more quickly.

Rotor bar breaking

Therefore, it is worth to employ diagnostic techniques to establish with good approximation if the conditions of the cage can ensure the operation of the motor with a sufficient degree of safety.

In practice, motors with a limited number of broken bars are usually still able to perform their operation without evident anomalies, as increased mechanical vibration or lengthening of the run-up time.

As a consequence of the asymmetry of the rotor electric circuit produced by this failure, the stator currents become unbalanced and with higher harmonic content, due to the presence of backward sequence components.

Rotor bar breaking

These phenomena arouse a sinusoidal torque oscillation, in addition to the constant torque, and gives rise to a spectral component in the stator current.

The amplitude of this spectral component of the stator current, which occurs due to the breakage of a single rotor bar, is often in the order of magnitude of that induced by the intrinsic constructive asymmetries of a healthy machine, and therefore it is difficult to distinguish between the two cases .

However, the motor does not remain in these conditions for a long time, since the aging process is greatly accelerated and therefore it is expected that the machine becomes unavailable in a short time.

Asymmetric rotor

With a healthy and symmetric rotor, the electromotive force induced in the rotor circuit have sf frequency, where s is the slip (arrow from f to sf).

The presence of an asymmetry in the rotor electric circuit determines a backward rotor field with a rotor current component at frequency -sf.

The stator "sees" a backward rotating rotor field at frequency:

$-sf_1 + (1-s)f_1 = f_1 - 2sf_1 = (1-2s)f_1$

This backward rotating rotor field induces an electromotive force in the stator, and hence a stator current component I_{left} at frequency (1-2s)f : arrow from -sf to (1-2s)f.

The stator current component I_{left} , induced by the rotor asymmetry, interacts with the rotor current component at frequency -sf: arrow from (1-2s) f to -sf.

Asymmetric rotor

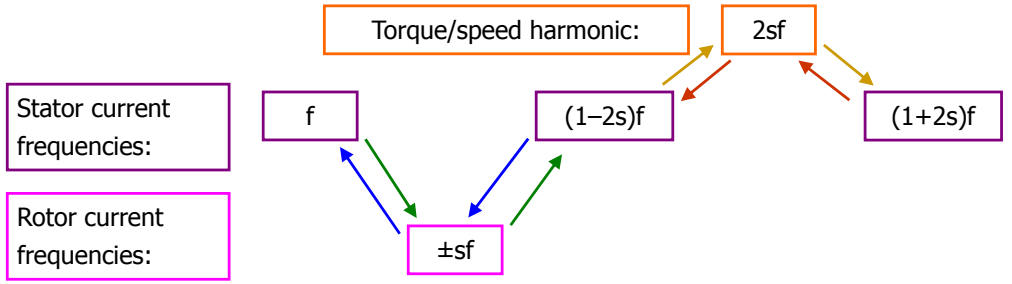

These phenomena also produce an oscillating torque at twice the slipping frequency (2sf) which gives rise to a ripple in the rotational speed, and consequently to an amplitude reduction of the stator current component I_{left} at frequency (1-2s)f.

As a further effect, the rotational speed oscillating phenomenon produces another stator current component I_{right} at frequency (1+2s)f.

Motor current signature analysis

So, the left current component is directly related to the rotor failure, while the right current component is caused by the speed ripple effect and its amplitude varies with the value of the combined rotor-load inertia. The effect of the speed ripple also affects the amplitude of the left current component.

The diagnostic procedure based on the current sidebands analysis at frequencies (1±2s)f is successful, especially if inter-bar currents are not present.

In the following, the experimental results related to a motor with aluminium die-cast rotor, 1.5 kW, 220 V, 50 Hz, 4 poles, nominal slip 6%, 28 rotor bars are presented. Three rotors were tested: i) healthy, ii) with one broken bar, iii) with two broken bars.

A. Bellini C. Concari, G. Franceschini, C. Tassoni, A. Toscani, "Vibrations, currents and stray flux signals to asses induction motors rotor conditions, IEEE Industrial Electronics", in *Proc. IECON 2006*.

Stator current spectrum

The amplitude of the sidebands at frequencies (1±2s)f in the stator current spectrum depends on:

- number of broken bars (increases with the number);
- load percentage (increases with the load).

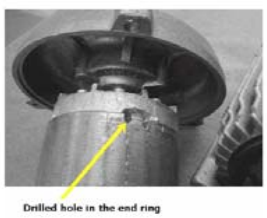

a) at no-load
b) at half load
c) at full load

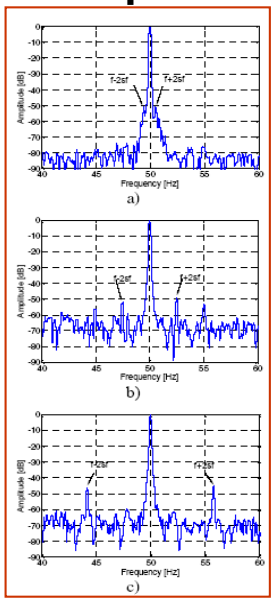

1 broken bar

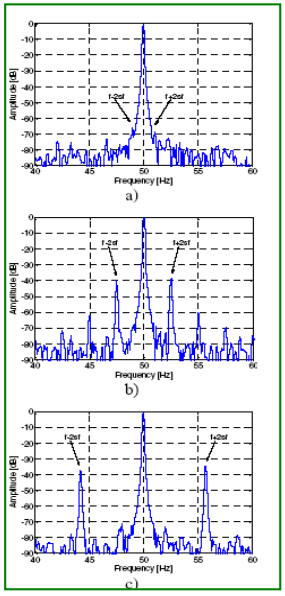

2 broken bars

Oscillating torque

Unfortunately, an oscillating torque can be even produced directly from the load, without the presence of rotor asymmetries or rotor failures.

These torque oscillation produces sidebands in the stator current spectrum which, in some cases, may appear at the same frequencies due to the broken rotor bars.

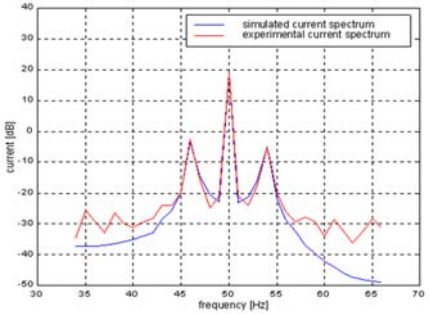

Therefore, for a more in-depth (but also more expensive) diagnostic analysis, it may be useful to consider other electromagnetic and mechanical parameters, measured by flux sensors, accelerometers and temperature transducers.

Radial vibration spectrum

Even the amplitude of the sidebands at frequencies $f_r \pm 2sf$ in the spectrum of the radial vibration depends on:

- number of broken bars (increases with the number);
- load percentage (increases with the load).

a) at no-load
b) at half load
c) at full load

Red: healthy Blue: faulty

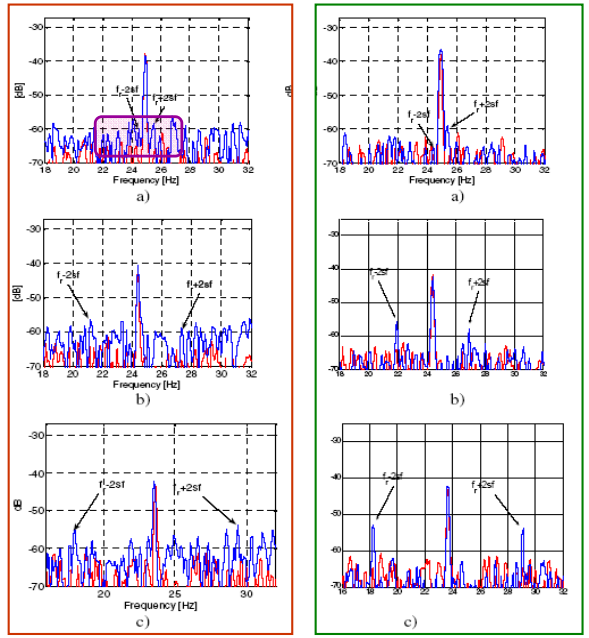

1 broken bar **2 broken bars**

External stray flux

In the same experimental tests, the e.m.f. induced by the external stray flux has been measured by means of a sensor consisting of 300 turns wound on a C-shaped magnetic core of rectangular cross-section (25x10 mm^2), positioned on the motor frame.

The external stray flux is the magnetic flux that radiates outside of the motor frame. Its magnitude is related to the place where the sensor is located around the machine body.

It is induced by both the stator and rotor currents, even if stator currents prevail, due to the magnetic shield effect provided by the stator against the rotor currents. Specifically, one or two stator phase currents dominate, due to the fixed position of the sensor and the distribution of the three-phase stator winding.

External stray flux

Therefore it is expected that stray flux includes the same information obtained by the stator current.

In fact, the sideband components at frequencies $f \pm 2sf$ are still present. As before, their amplitudes depend on the machine load.

Notice that the right side component amplitude increases with slip more than the left one because the e.m.f., i.e. the flux derivative, is used instead of the flux.

2 broken bars

a) at no-load
b) at half load
c) at full load

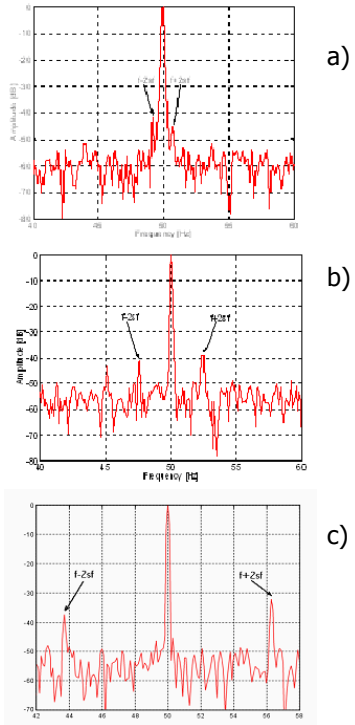

External stray flux

In summary, stator current and stray flux signals can be used with the same effectiveness in order to detect and quantify rotor faults.

The optimal choice depends on the specific application and on the easiness of installing flux or current sensors in the specific industrial environment.

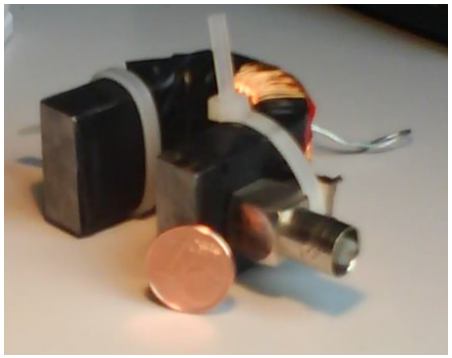

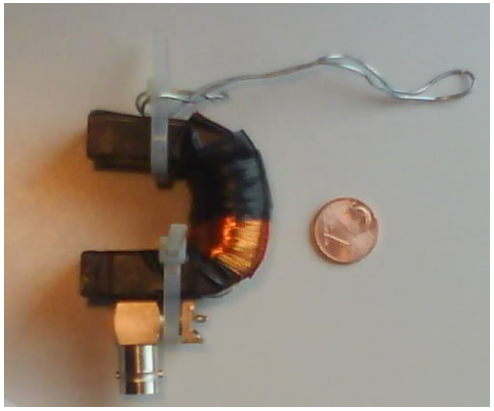

Rotor bar skewing and its effects

Pros:

- Reduction of torque ripple (reduction of the parasitic torques and the consequent risk of cogging during the startup)
- Noise reduction during the normal operation

Cons:

- Increase of the **inter-bar currents**

Rotor bar skewing and its effects

The inter-bar current is the current flowing between adjacent bars of a cage rotor, through the magnetic iron core, which produces a non-uniform distribution of the current along the axial length of the machine.

Since there is no insulation between bar and core, only the bar-core contact resistance limits the current flowing in the core.

Some researches have highlighted that this contact resistance is about 70 times greater than the iron resistance.

In the classical theory of induction machines, the inter-bar currents are generally neglected.

The usual assumption is that aluminium (or copper) bar resistance is much lower than iron core resistance and bar-core contact resistance, so the current completely flows along the bars.

Rotor bar skewing and its effects

On the contrary, several experimental studies have proven that current flows also between adjacent bars through the iron core.

This phenomenon is accentuated in skewed cage rotors because the natural path for the rotor current is along the axial length of the bar, but it is forced along the skewed bar direction.

In fact, in an induction motor, the magnetic flux is radial, the induced electromotive force on the rotor is axial and therefore also the current should be axial.

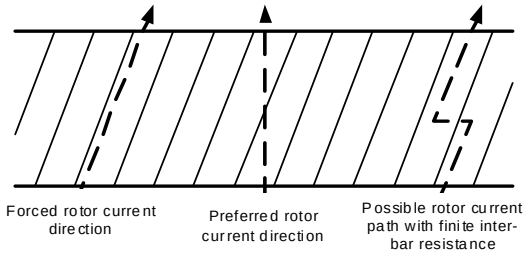

Rotor bar skewing and its effects

Other researches have shown that:

- ✓ Resistivity between bars is lower in case of copper die-cast rotors than aluminum die-cast rotors;
- ✓ Inter-bar currents become remarkable when a bar is broken.

If inter-bar currents are relatively high in a healthy motor, then, in case of broken bar, the current flowing between the adjacent bars to the broken one (near to the short circuit ring, where the break is present) will become even higher, causing a chain reaction that could more easily break the adjacent bars.

From a diagnostic point of view, these high inter-bar currents can reduce the imbalance caused by a broken bar: this effect can make harder the early detection of the broken bar, when the sidebands currents around the fundamental are monitored.

Effect of the inter-bar currents on the diagnostics

The diagnostic procedure based only on the stator current analysis for the detection of a broken rotor bar may fail if remarkable inter-bar currents are present, since they reduce the degree of asymmetry of the rotor and, consequently, the amplitude of the considered spectral components.

On the other hand, the presence of inter-bar currents has a further effect on the rotor vibrations: the interaction of the radial magnetic flux with the inter-bar currents, which flow tangentially along the rotor circumference, produces a force (and hence a vibration) in the axial direction.

Therefore, the analysis of the previously considered parameters (stator current, stray flux, radial vibrations) together with the axial vibration can increase the effectiveness of the proposed diagnostic procedure.

Effect of the inter-bar currents on the diagnostics

C. Concari, G. Franceschini, C. Tassoni, "Differential diagnosis based on multivariable monitoring to assess induction machine rotor conditions", *IEEE Trans. on Industrial Electronics*, Vol. 55, No. 12, 2008.

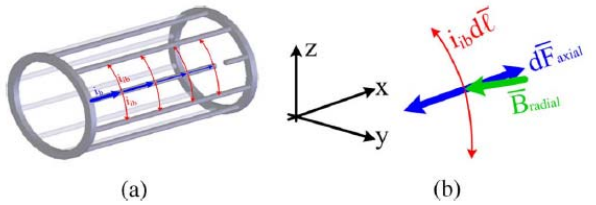

Fig. 8. Interbar currents in case of (a) bar breakage and (b) generation of an axial force.

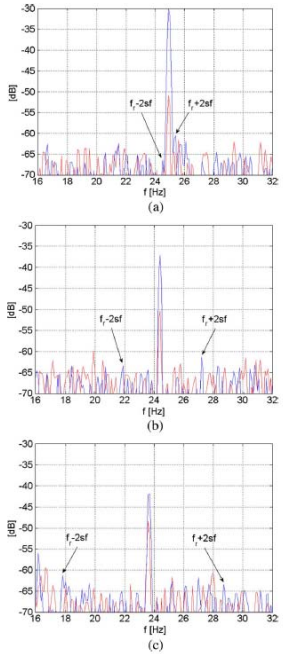

Fig. 19. Axial vibration signal spectra in the range close to f_r (blue two broken bars, red healthy) (a) no load, (b) half load, and (c) full load.

Effect of the inter-bar currents on the diagnostics

The graphs in the previous slide refer to a small induction motor (1.5 kW, 4 poles) with die-cast aluminium cage: in this case, the currents between bars in presence of one or two broken bars are negligible and the rotor diagnosis by means of the stator current analysis is still effective.

Another research has considered a higher power motor (55 kW, 2 poles, with copper cage and skewed bars) and has verified that a broken bar modifies the axial vibrations at particular frequencies.

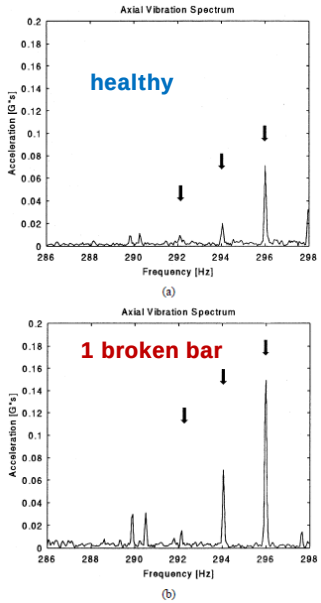

G.H. Muller, C.F. Landy, "A novel method to detect broken rotor bars in squirrel cage induction motors when interbar currents are present", *IEEE Trans. on Energy Conversion*, Vol. 18, Issue 1, 2003.

Airgap eccentricity

Airgap eccentricity causes a force called Unbalanced Magnetic Pull (UMP) on the rotor that tries to pull the rotor even further from the stator bore centre, in the direction of the minimum airgap. If the levels of eccentricity are not kept within specified limits (typically a maximum of 10%), then eccentricity can cause excessive stressing of the motor and can increase bearing wear.

Moreover, the radial magnetic force waves produced by eccentricity act on the stator core assembly and rotor cage and thus subject the stator and rotor windings to potentially harmful vibrations. Besides, acoustic noise levels can substantially increase.

High UMP due to severe airgap eccentricity can ultimately lead to a rotor to stator rub, with consequential damage to the stator core, stator windings and rotor cage. This can cause insulation failure of the stator winding or breaking of the rotor cage bar or end rings and, hence, a costly repair, in case of a high voltage induction motor.

Airgap eccentricity

Airgap eccentricity can occur due to manufacturing tolerances, installation procedures (in large motors), other damages or wear and tear.

When the rotor can be considered as rigid and the motor is equipped with rolling bearings, as in the most induction motors, the airgap eccentricity can be distinguished in two types, static and dynamic, which can exist simultaneously (mixed eccentricity).

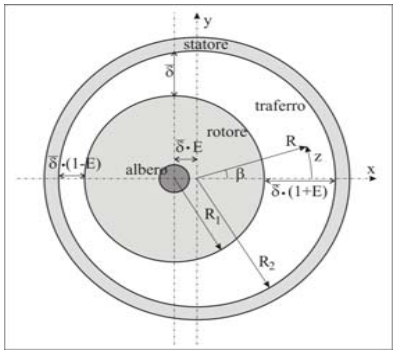

Static eccentricity

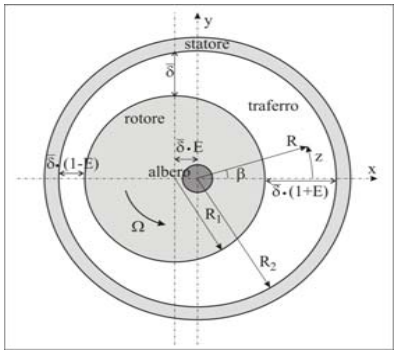

Dynamic eccentricity

Static eccentricity

Static eccentricity:

The rotor rotates around its axis, which coincides with the shaft axis, but does not coincide with the stator axis.

The rotor is symmetrical to its axis, so there is no mechanical imbalance.

Static eccentricity can be caused by a misalignment due to constructive tolerances, bearings wear, stator core ovality or incorrect positioning of the rotor or stator.

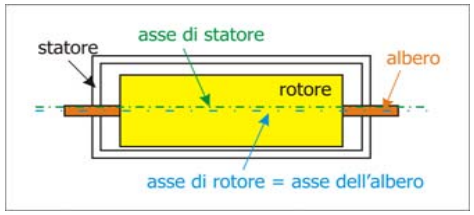

The minimum radial airgap length is fixed in space.

Dynamic eccentricity

Dynamic eccentricity:

The rotor rotates around the stator axis but not around its axis.

The shaft axis does not coincide with the rotor shaft.

Therefore, dynamic eccentricity arouses also a mechanical imbalance, i.e. a centrifugal force rotating at the rotor rotational speed.

It can be caused by incorrect manufacturing (nonconcentric outer rotor diameter), rotor thermal bowing, bearing wear and movement or rotor flexible behavior.

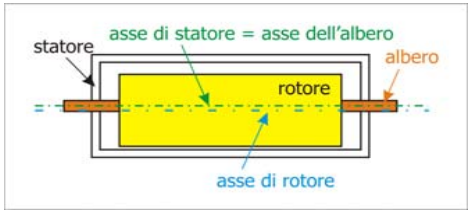

The minimum airgap revolves with the rotor and is a function of space and time

The Maxwell stress tensor

In order to understand what happen in case of eccentricity, it is necessary to calculate the Maxwell stress tensor. The force per unit of surface which tends to close the gap between two blocks of ferromagnetic materials is defined by the radial component of the Maxwell stress tensor and can be expressed in terms of flux density B, whose lines are perpendicular to the airgap surfaces:

$$\sigma_n = \frac{F_n}{S} = \frac{B^2}{2\mu_0} \qquad \left[\frac{V^2 \cdot s^2 / m^4}{V \cdot s / A \cdot m} = \frac{V \cdot s \cdot A \cdot m}{m^4} = \frac{N \cdot m^2}{m^4} = \frac{N}{m^2} \right]$$

In case of a perfectly concentric rotor and stator, these forces act perpendicularly and symmetrically on the rotor and stator surfaces, so that their resultant is null on the overall circumference.

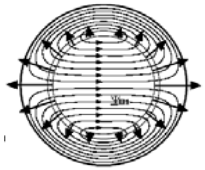

The Maxwell stress tensor

In induction machines, the magnetic flux Φ at the airgap is determined by the interaction between the magnetomotive forces produced by the stator and rotor windings and it is proportional to the overall m.m.f. *M*.

In a simplified explanation of the problem, we can consider these magnitudes linked by the simple relationship:

$$\Phi = \frac{M}{\Re}$$

where $\Re$ is the reluctance of the magnetic circuit in which the flux Φ flows.

Since the reluctance of the airgap is much higher than that of the iron core, the latter is neglected in the approximated calculation of the m.m.f. required to produce a certain flow Φ.

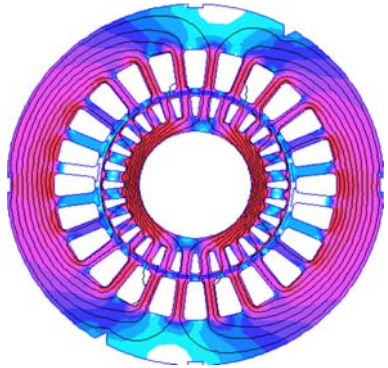

The Maxwell stress tensor

$$\Re \cong \Re_{airgap} = \frac{2\delta}{\mu_0 S}$$

$$M = \Phi\Re = B \cdot S \frac{2\delta}{\mu_0 S} = \frac{B \cdot 2\delta}{\mu_0}$$

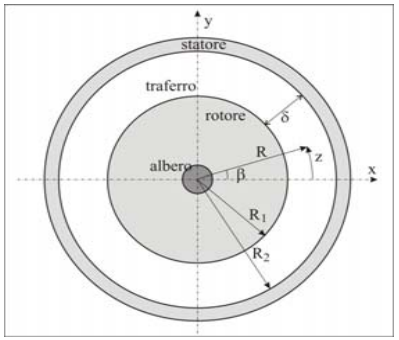

B = flux density at the airgap [T]

μ_0 = magnetic permeability of the air [H/m]

δ = airgap length [m]

S = any perpendicular surface crossed by the flux [m²]

The Maxwell stress tensor

The main harmonic component of the m.m.f. *M* has a sinusoidal spatial distribution at the airgap, with a period depending on the number of pole pairs p_p , and an amplitude which is sinusoidally variable over the time according to the supply frequency *f*:

$$M_1(\beta, t) = \overline{M}_1 \cos(\omega t - p_p \beta) \qquad \beta = \frac{z}{R} \qquad \omega = 2\pi f$$

As a consequence, even the amplitude of the main harmonic component of the flux density *B* is sinusoidally variable over the time according to the supply frequency *f*:

$$B(\beta, t) = \underbrace{\frac{\mu_0 \overline{M}_1}{2\delta}}_{\overline{B}} \cos(\omega t - p_p \beta) = \overline{B} \cos(\omega t - p_p \beta)$$

The Maxwell stress tensor

The radial component of the Maxwell stress tensor is proportional to the square of the flux density B:

$$B^2(\beta,t) = \overline{B}^2 \cos^2(\omega t - p_p \beta)$$

Knowing that:

$$\cos^2(\alpha) = \frac{1}{2}(\cos(2\alpha)+1)$$

We obtain:

$$B^2(\beta,t) = \frac{1}{2}\overline{B}^2 \cos(2\omega t - 2p_p\beta) + \frac{1}{2}\overline{B}^2$$

Therefore, the radial force due to the Maxwell stress tensor has a component which is sinusoidally variable over the time with twice the supply frequency.

The Maxwell stress tensor

For this reason, the main frequency of the stator case vibration is twice the supply frequency (100 Hz in Europe), even when rotor and stator are perfectly concentric each other.

By integrating the Maxwell stress tensor throughout the airgap, a null resultant is obtained, both in horizontal and vertical direction:

$$F_x = \int_0^{2\pi} \frac{B^2(\beta,t)}{2\mu_0} \cos\beta d\beta = 0 \qquad F_y = \int_0^{2\pi} \frac{B^2(\beta,t)}{2\mu_0} \sin\beta d\beta = 0$$

This is valid in case of perfect symmetry between rotor and stator.

Let's see what happens when the rotor and stator are not concentric (skipping some passages of the demonstration).

Static eccentricity

In case of static eccentricity, the airgap length is given by:

$$\delta(\beta) = \overline{\delta} \cdot (1 + E\cos\beta)$$

But in the expression of the flux density there is the inverse of δ, therefore the calculation becomes quite complicate. The result is:

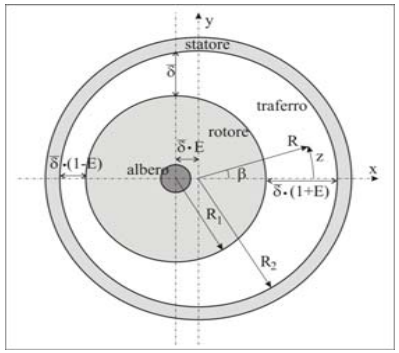

$$B(\beta,t) = B_1\cos(\omega t - p_p\beta) + B_2\cos(\omega t - (p_p-1)\beta) + B_2\cos(\omega t - (p_p+1)\beta)$$

a component with p_p pole pairs, as in case of concentric rotor

a component with (p_p-1) pole pairs

a component with (p_p+1) pole pairs

Effect of static eccentricity on vibrations

In presence of static eccentricity, the flux density is given by the interaction of three harmonics with different number of pole pairs.

In case of static eccentricity, by integrating the Maxwell stress tensor throughout the airgap, a non-null resultant in the direction of the minimum airgap is obtained: the steady Unbalanced Magnetic Pull (UMP).

Besides, it can be proven that static eccentricity produces an additional component of the radial force (with respect to the concentric rotor condition) which sinusoidally varies over the time with twice the supply frequency.

Therefore, a vibration increase at 100 Hz (if the supply frequency is 50 Hz) can be expected in presence of static eccentricity.

Effect of static eccentricity on vibrations

Example of approximate distribution of the flux density B:

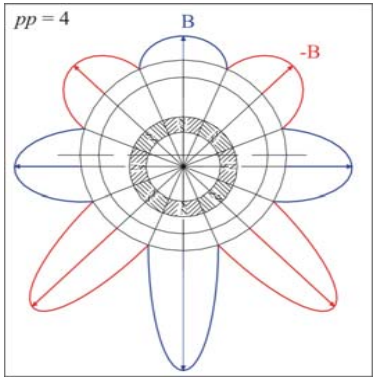

Corresponding distribution of the radial force (proportional to the square of B):

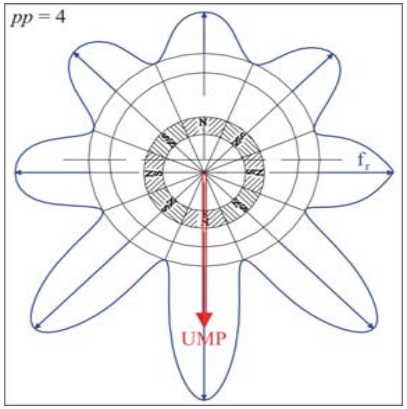

UMP = Unbalanced Magnetic Pull

Dynamic eccentricity

In case of dynamic eccentricity, the distribution of the airgap rotate at the rotational speed of the rotor Ω, therefore the length of the airgap can be expressed as:

$$\delta(\beta,t) = \bar{\delta} \cdot (1 + E\cos(\beta - \Omega t))$$

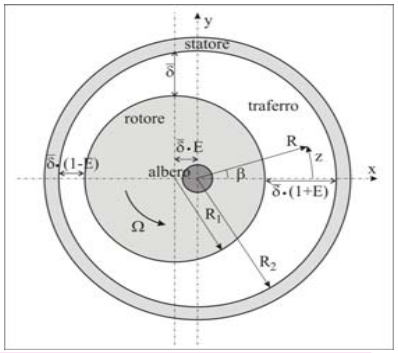

Dynamic eccentricity produces a magnetic rotating force (rotating UMP) at the rotational rotor speed Ω (frequency f_r), which is added to the centrifugal force due to the mechanical unbalance (at the same frequency).

Effect of eccentricity on vibrations

By using the expression of the airgap length in presence of dynamic eccentricity, it is possible to calculate the flux density B, similarly to the case of static eccentricity, and hence the Maxwell stress tensor, which is proportional to the square of B.

In this way, it can be found that dynamic eccentricity also produces vibrations at the following frequencies (sidebands around the fundamental):

$$2f_s - f_r \qquad 2f_s + f_r$$

By summarizing, for the induction motors it has been proven that the amplitude of the **vibration harmonics** at frequencies: $2f_s$, f_r, $2f_s \pm f_r$

- rapidly increases with both static and dynamic eccentricity, especially at no-load;
- static eccentricity has only a slight influence on the component at f_r, which, on the other hand, is caused by both the rotating UMP and the mechanical imbalance (both arising from dynamic eccentricity).

MCSA to detect rotor eccentricity

Regarding the MCSA, for the induction motors it has been proven that the amplitude of the **current harmonics** at frequencies: $f_s \pm f_r$

- Is strongly dependent on the degree of both static and dynamic eccentricity;
- The effect of the dynamic eccentricity increases from the full load operation to the no-load condition.

D.G. Dorrell, W.T. Thomson, "Analysis of airgap flux, current, and vibration signals as a function of the combination of static and dynamic airgap eccentricity in 3-phase induction motors", *IEEE Trans. Ind. Appl.*, vol. 33, no. 1, 1997, 24-34.

Further current harmonics at frequencies which depends also on the number of rotor slots have been proposed to detect rotor eccentricity and proven to be function of the combination of static and dynamic eccentricity.

J.R. Cameron, W.T. Thomson, A.B. Dow, "Vibration and current monitoring for detecting airgap eccentricity in large induction motors", *IEE Proceedings B - Electric Power Applications*, vol. 133, no. 3, May 1986.
W. T. Thomson, R. J. Gilmore, "Motor current signature analysis to detect faults in induction motor drives – fundamentals, data interpretation, and industrial case histories", in *Proc. Thirty-Second Turbomachinery Symposium*, Houston, Texas, Sept. 2003.

Short circuits in stator winding supplied at LV

Short circuits in stator winding can occur:

1) between turns of the same phase (**turn-to-turn**);

2) between turns of different phases (**phase-to-phase**);

3) between turns and stator core (**phase-to-ground**).

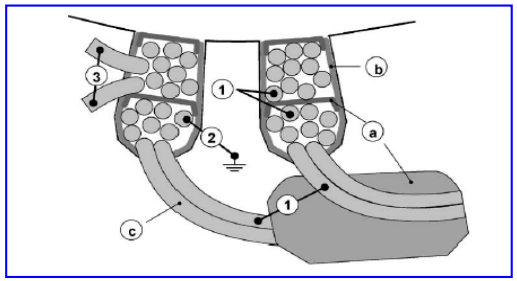

1) Phase-to-phase voltage
2) Phase-to-ground voltage
3) Turn-to-turn voltage

a) Phase insulation
b) Ground insulation
c) Turn insulation

Short circuits in stator winding supplied at LV

1) Short circuit between turns of the same phase:

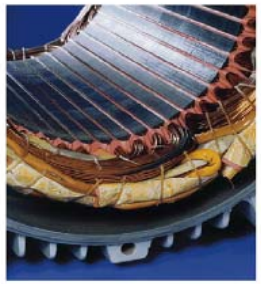

2) Short circuit between different phases:

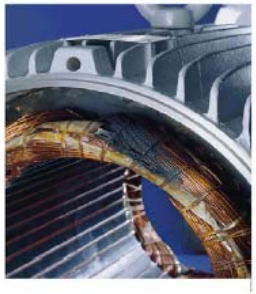

3.a) Short circuit between turns and stator core at the end of the slot:

Short circuits in stator winding supplied at LV

3.b) Short circuit between turns and stator core in the middle of the slot :

Short circuit on the connections:

Short circuit of the overall winding:

Short circuits in stator winding supplied at LV

Generally, a stator winding insulation failure begins with a short circuit between turns that involves few turns within the same coil.

With a **turn-to-turn** short circuit, the motor can continue to run, but for how long?

This short circuit generates a high circulation current in the short circuited turns, which causes localized heating and favors a rapid diffusion of the fault to a greater section of the winding.

If not detected, the fault between the turns can propagate and cause **phase-to-phase** or **phase-to-ground** failures.

With phase-to-phase or phase-to-ground short circuit, the motor cannot operate and the protective devices disconnect it from its power supply.

Diagnostics of short circuits at LV

In low-voltage machines, the time between a **turn-to-turn** short circuit and a **phase-to-phase** or **phase-to-ground** short circuit can take few minutes or few hours, depending on the severity of the fault and on the motor load. So this is a quickly progressive fault.

To avoid **phase-to-phase** or **phase-to-ground** short circuits in low-voltage machines, the only solution is to detect the **turn-to-turn** short-circuits through an online diagnostic technique.

For LV machines, many manufacturers and operators argue that there is no diagnostic tool that is worth being used to detect **turn-to-turn** short circuits: their idea is that, if a motor starts to fail, it will continue to work until it will breakdown and therefore it will be substituted.

But this principle could be valid only if the failure of the motor will not damage the rest of the system and if there is a spare part of the same motor immediately ready to start to work.

Diagnostics of short circuits at LV

In fact, in some cases, an unexpected failure of a low power LV motor can be very expensive or can cause serious safety hazards.

Therefore, even for LV machines, it may be useful to develop a diagnostic tool that allows to early detect a short circuit, in order to plan in advance the replacement of the machine and to avoid more heavy failures.

The literature on this subject has identified as possible indicators of stator short circuits for LV machines:

- the stator current (MCSA), which can be measured by means of a non-invasive instrument as a current probe;
- the stray electromagnetic flux, which can be collected by means of an external flux sensor.

Diagnostics of short circuits at LV

It is important to observe that, among the on-line diagnostic techniques which can be employed to early detect a potential short circuit in a winding of an electrical machine, there is a clear distinction between:

- ✓ the partial discharge (PD) monitoring to diagnose the insulation degradation prior to fault in High Voltage (HV) machines;
- ✓ the MCSA to detect shorted turns in Low Voltage (LV) induction motors.

Note that HV machines are normally related to an electrical supply with rated voltage ≥ 700 V, whereas LV machines refer to rated voltage <700 V: under sinusoidal power conditions, the insulation systems of LV machine are not subject to partial discharges.

Flux and current sensors

There are commercial flux sensors which can be used together with (or instead of) current probes:

Axial flux measurement set up used in this thesis.

V. Kokko, "Condition monitoring of squirrel-cage motors by axial magnetic flux measurements", Academic Dissertation, University of Oulu, 2003.

Both sensors must allow the frequency analysis of the acquired signals.

Further custom flux sensors can be realized in laboratory.

Characteristic frequencies proposed for the diagnostics of the stator short circuits by means of current and stray flux analysis

Author	Characteristic frequencies
Penman et al.	$f_s\left(k \pm n\frac{1-s}{p}\right) = kf_s \pm nf_r$
Stavrou et al.	$(f_s - f_r)$ $f_s\left(N_r \frac{1-s}{2p} + 2 + 1\right)$
Thomson	$f_s\left(n\frac{1-s}{p} \pm k\right) = nf_r \pm kf_s$
Henao et al.	$f_s\left(\gamma \frac{N_r}{p}(1-s) \pm \nu\right)$
Cruz and Cardoso	$3f_s$
Romary et al.	$15f_s$, $17f_s$

- ✓ J. Penman, H.G. Sedding, B.A. Lloyd, W.T. Fink, "Detection and location of interturn short circuits in the stator windings of operating motors," *IEEE Trans. Energy Convers.*, vol. 9, no. 4, pp. 652-658, 1994.
- ✓ A. Stavrou, H.G. Sedding, J. Penman, "Current monitoring for detecting inter-turn short circuits in induction motors," *IEEE Trans. Energy Convers.*, vol. 16, no. 1, pp. 32-37, Mar. 2001.
- ✓ W.T. Thomson, "On-line MCSA to diagnose shorted turns in low voltage stator windings of 3-phase induction motors prior to failure," in *Proc. IEMDC 2001*, pp. 891–898.
- ✓ H. Henao, C. Demian, G.A. Capolino, "A frequency-domain detection of stator winding faults in induction machines using an external flux sensor," *IEEE Trans. Ind. Appl.*, vol. 39, no. 5, pp. 1272-1279, 2003.
- ✓ S.M.A. Cruz, A.J.M. Cardoso, "Diagnosis of stator inter-turn short circuits in DTC induction motor drives," *IEEE Trans. Ind. Appl.*, vol. 40, no. 5, pp. 1349-1360, 2004.
- ✓ R. Romary, R. Pusca, J. P. Lecointe, J. F. Brudny, "Electrical machines fault diagnosis by stray flux analysis," in *Proc. WEMDCD 2013*, pp. 245–254.

f_s = supply frequency
f_r = rotational frequency
p = number of pole-pairs
s = slip
N_r = number of rotor bars

k = odd integer positive number (k = 1, 3, 5, ...)
n = integer positive number (n = 1, 2, 3, … 2p-1)
γ = integer positive or null number (γ = 0, 1, 2, 3, …)
ν = harmonic index of the stator current

Short circuits detection with current and flux

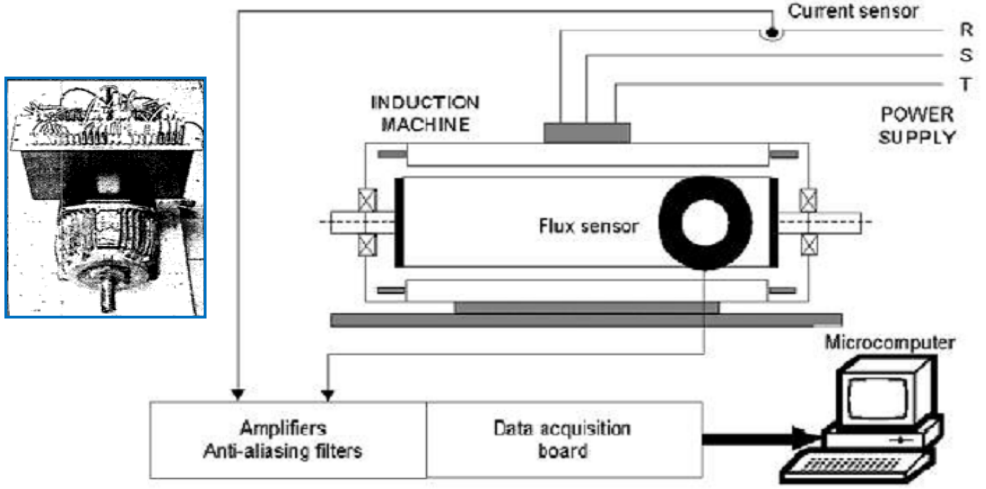

H. Henao, C. Demian, G.A. Capolino, "A frequency-domain detection of stator winding faults in induction machines using an external flux sensor", *IEEE Trans. Ind. Appl.*, 39(5), pp. 1272-1279, 2003.

Short circuits detection with current and flux

The efficiency of the stator winding fault detection based on the stray flux and stator current analysis was tested on an induction motor, 11 kW, 230/400 V, 50 Hz, 4 poles.

A stray flux sensor and a stator current probe have been connected to the same data acquisition board through two voltage amplifiers, to scale the magnitude of the signals, and through two low-pass anti-aliasing filters, to set the frequency bandwidth to a correct range.

The current and the stray flux have been analyzed in both the time and frequency domain, initially at standstill.

The power supply can be given by the grid or by a VSI, in order to test the robustness of the proposed method in presence of other harmonics coming from the voltage source and not from the motor itself.

Short circuits detection with current and flux

The data acquisition board is set for a 250 kHz sampling rate, with low-pass anti-aliasing filters, having a cutoff frequency of 2 kHz.

The current probe is a Rogowski coil with an external analog amplifier.

The stray flux sensor is a 1000 turns air coil, placed near the machine body and connected to a voltage analog amplifier with variable gain.

The motor has been rewound with a phase parallel circuit having the first turns (from 1 to 6) being accessible from the outside.

This arrangement allows to perform a short circuit in the same phase at a reasonable level (from 1% to 6%).

The short circuit current in the winding is limited by an adjustable resistance to keep it not higher than the rated value, for steady-state measurements.

Analysis in the time domain of current and flux

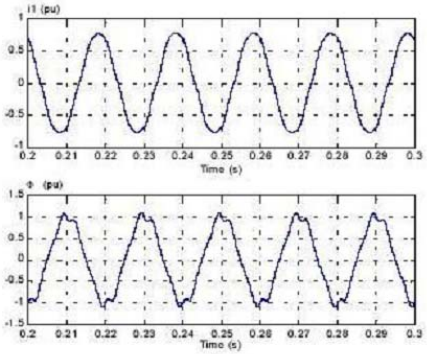

a) without fault

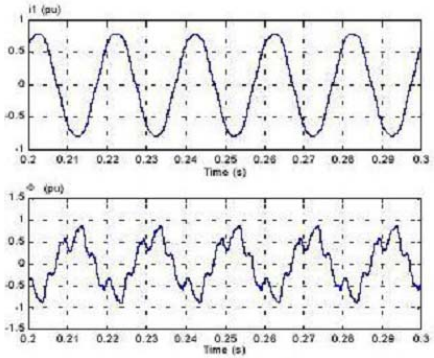

b) with fault

At the top: stator current.

At the bottom: stray flux.

Motor at standstill connected directly to the grid

The stray flux shows greater distortion when the fault is present.

In this case, the analysis in the time domain is sufficient to detect the fault.

Analysis in the time domain of current and flux

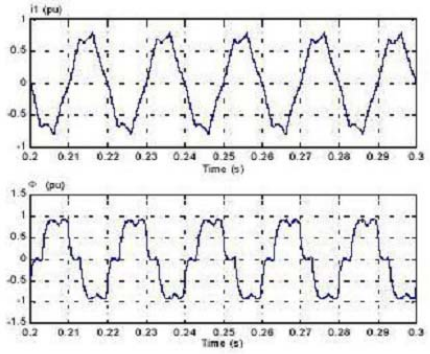

a) without fault

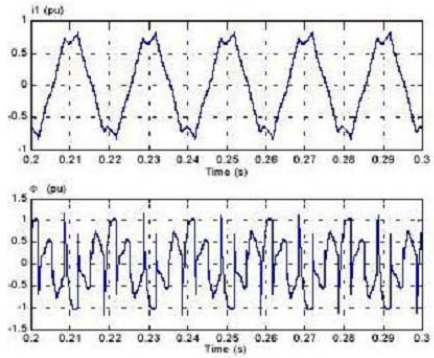

b) with fault

At the top: stator current.

At the bottom: stray flux.

Motor at standstill connected to the VSI

By supplying the motor with a VSI, at the same fundamental frequency, the distortion of the flux increases more than the current.

Analysis in the frequency domain

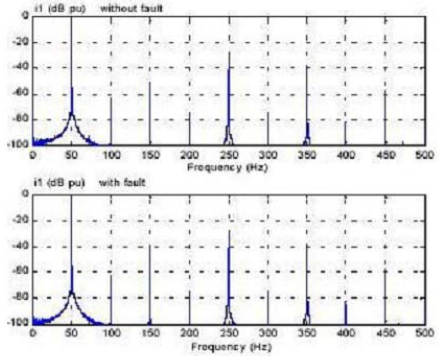

a) Stator current

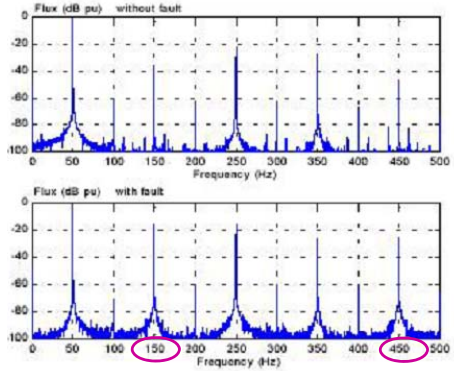

b) Dispersion flux

At the top: healthy. At the bottom: faulty.

Motor at standstill connected directly to the grid

The current seems not sensible to the fault.

The two stray flux spectra are very different: the fault is identified by the increase of the harmonics at 150 Hz and 450 Hz.

Analysis in the frequency domain

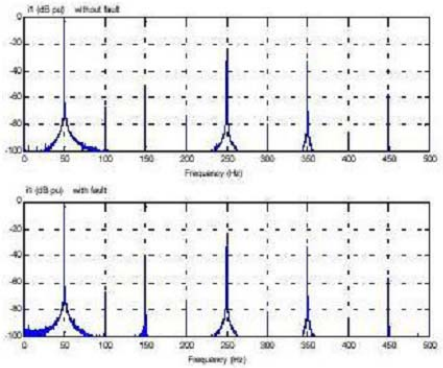

a) Stator current

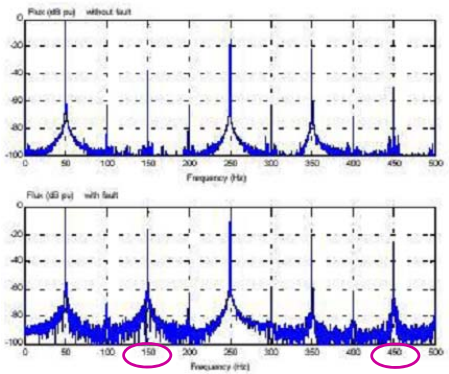

b) Dispersion flux

At the top: healthy. At the bottom: faulty.

Motor at standstill connected to the VSI

Again, the current seems not sensible to the fault, whereas the stray flux spectra are very different: the fault is still identified by the increase of the harmonics at 150 Hz and 450 Hz.

Analysis in the frequency domain

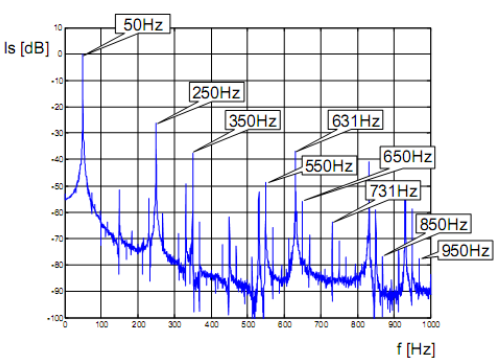

Current

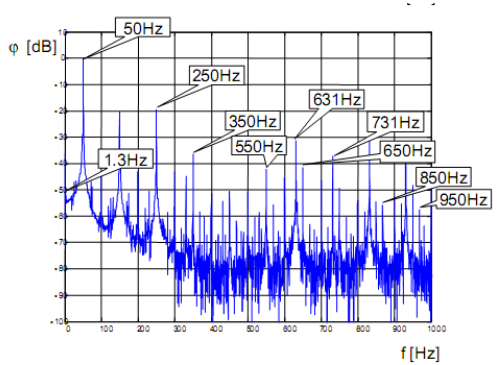

Flux

These are the normalized spectra during the operation at rated load, with the healthy motor.

Analysis in the frequency domain

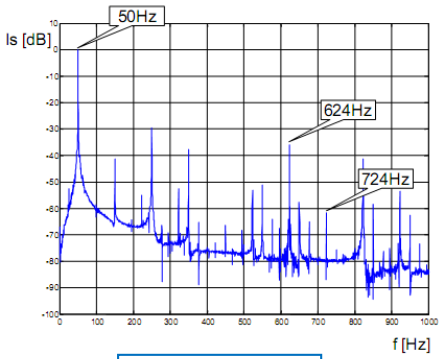

Current

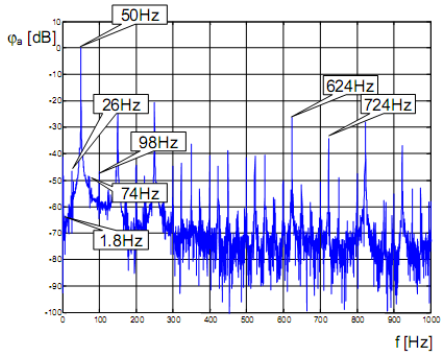

Flux

These are the normalized spectra during the operation at rated load, with the the 6% of short-circuited turns.

Note that rotor speed decreases, due to the fault, as the electromagnetic torque produced by the motor decreases.

Short circuits detection with current and flux

This method was initially tested with the motor at standstill, and then rotating, from no-load to the rated load.

In the latter case, the number of excited harmonics increases and the fault detection becomes more complex.

In general, this technique is quite easy to implement and can use low cost tools.

It looks promising for an industrial application, as it is non-invasive and it does not require any particular precaution for its installation.

Nevertheless, the effectiveness of the diagnostic techniques to detect short circuits in low voltage motors has still to be proven and, above all, it is necessary to evaluate each time the economic convenience of the application of these techniques.

Bearing faults

Bearing faults can happen due to the following main causes:

- ❑ Normal fatigue (wear and tear);
- ❑ Contamination (airborne dust, dirt or any abrasive substance);
- ❑ Improper lubricant or poor lubrication;
- ❑ Corrosion (corrosive fluids or corrosive atmosphere)
- ❑ Shaft voltage (bearing currents)
- ❑ Excessive load
- ❑ Misalignment
- ❑ Overheating

Most of these causes (but not all) arouse slowly progressive bearing faults.

Periodical vs. predictive maintenance

For this reason, the **common practice** to detect bearing faults in low voltage motors is a combination of:

- a **periodical condition monitoring** of the motors, in which expert technicians collect and elaborate vibration measurements by means of sensors not permanently installed on the machines;
- a **periodical preventive substitution** of the bearings after a given number of hours indicated by the manufacturer.

This periodical maintenance is generally effective, but:

- it is **expensive** and normally needs the employment of personnel and instruments **external** to the firm;
- it can require early unnecessary substitution of bearings;
- **can fail** in case of quickly progressive faults, as those due to shaft currents caused by electronic converters.

Periodical vs. predictive maintenance

For these reasons, over recent years, many studies have been focused on the implementation of a **predictive condition monitoring** scheme able to detect bearing faults in their incipient stage by means of on-line continuous measurement and analysis of variables **easy to collect**, **non-invasive** and **low cost**:

- vibration, → well consolidated methodology for these faults
- current,
- stray flux.

This detection scheme needs to categorize bearing faults into two main groups:

- **single-point defects** (cyclic);
- **generalized roughness** (non-cyclic).

Single-point defects

A single-point defect produces an impact between the ball and the raceway and generates detectable **vibrations** at predictable frequencies f_v which depend on:

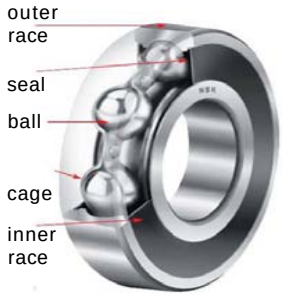

- surface of the bearing which contains the fault (outer race, inner race, ball, cage);
- geometrical dimensions of the bearing;
- rotational speed of the rotor f_r .

The theoretical frequency to monitor in the vibration spectrum to detect a fault in the outer race is:

$$f_o = \frac{N}{2} f_r \left(1 - \frac{d}{D}\cos\alpha\right)$$

N = number of rolling elements (ball or roll)
d = diameter of the rolling element
D = bearing pitch diameter
α = ball contact angle, often equals to 0°.

Single-point defects

To detect a fault in the inner race:

$$f_i = \frac{N}{2} f_r \left(1 + \frac{d}{D}\cos\alpha\right)$$

For a defect in the rolling elements:

$$f_b = \frac{D}{2d} f_r \left(1 - \left(\frac{d}{D}\right)^2 \cos^2\alpha\right)$$

For a defect in the cage:

$$f_c = \frac{1}{2} f_r \left(1 + \frac{d}{D}\cos\alpha\right)$$

For simplicity, the outer and the inner race characteristic frequencies can be approximated for most bearings by:

$$f_o = 0.4 \cdot N \cdot f_r \qquad f_i = 0.6 \cdot N \cdot f_r$$

Vibration analysis for single-point defects

Example of analysis of the vibrations in the frequency domain (inner race fault):

5: Frequency spectrum of envelope signal between 0 and 200 Hz, below: undamaged bearing; above: damaged bearing
n_{IR} Inner ring speed [min^{-1}]
f_{IR} Frequency of inner ring signal (cycling frequency) [Hz]

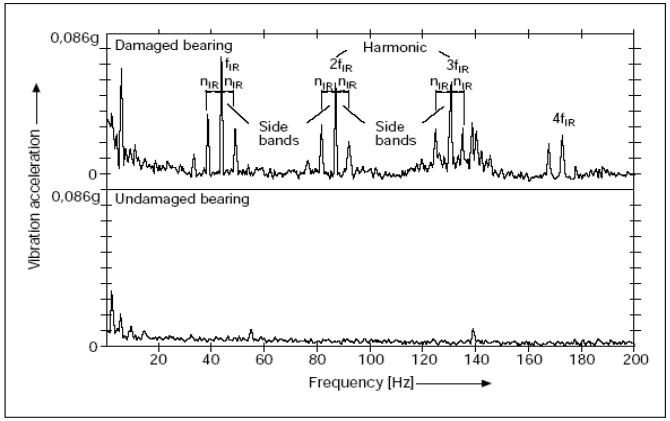

MCSA to detect bearing faults

The relationship between the bearing vibration and the stator current of an induction motor can be determined by remembering that any airgap eccentricity produces an asymmetry in the flux density at the airgap.

In turn, this asymmetry affects the inductances of the machine which determine the harmonics of the stator current.

Since rolling bearings support the rotor, any bearing defect produces a radial displacement between rotor and stator.

Therefore, the radial motion produced by a single-point defect arouses stator current components at predictable frequencies f_p :

$$f_p = \left| f_s \pm k f_v \right| \qquad f_s = \text{supply frequency}$$

where f_v is one of the characteristic vibration frequencies to detect a single-point defect and k = 1, 2, 3, …

MCSA to detect bearing faults

Since 1995, many studies have been focused on the possibility to employ the motor current signature analysis (MCSA) as an alternative diagnostic index for bearing faults, with respect to the vibration measurements.

After 2006, even the external stray flux has been considered with the same purpose.

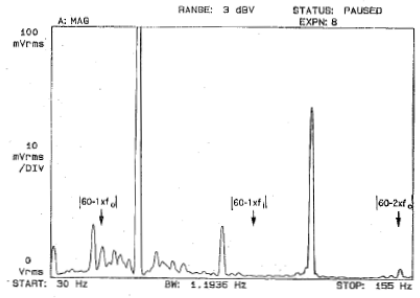

Fig. 4. Stator current spectrum of loaded 4-pole induction machine with a hole in the outer race of the shaft-end bearing (30–155 Hz).

- ✓ R. R. Schoen, T. G. Habetler, F. Kamran, and R. G. Bartheld, "Motor bearing damage detection using stator current monitoring," *IEEE Trans. Ind. Appl.*, vol. 31, no. 6, pp. 1274-1279, Nov./Dec. 1995.
- ✓ M. D. Negrea, "Electromagnetic Flux Monitoring for Detecting Faults in Electrical Machines," Ph.D. Thesis, Department of Electrical and Communications Engineering, Helsinki University of Technology, Espoo, Finland, 2006.

Generalized roughness

Generalized roughness is a very common fault in rolling bearings, but it has not been sufficiently considered in the literature.

Since generalized roughness is not a single-point defect, the characteristic fault frequencies f_p are not expected to be excited and their monitoring could be ineffective to detect this fault.

Only few studies have been dedicated to discover a generalized roughness by means of MCSA and none by means of the stray flux analysis.

- ✓ J. R. Stack, T. G. Habetler, and R. G. Harley, "Bearing fault detection via autoregressive stator current modeling," *IEEE Trans. Ind. Appl.*, vol. 40, no. 3, pp. 740-747, May/Jun. 2004.
- ✓ W. Zhou, B. Lu, T.G. Habetler, and R.G. Harley, "Incipient Bearing Fault Detection via Motor Stator Current Noise Cancellation Using Wiener Filter," *IEEE Trans. Ind. Appl.*, vol. 45, pp. 1309-1317, no. 4, Jul./Aug. 2009.
- ✓ A.M. Knight and S.P. Bertani, "Mechanical fault detection in a medium sized induction motor using stator current monitoring," *IEEE Trans. Energy Convers.*, vol. 20, no. 4, pp. 753 760, Dec. 2005.
- ✓ F. Immovilli, M. Cocconcelli, A. Bellini, and R. Rubini, "Detection of generalized-roughness bearing fault by spectral-kurtosis energy of vibration or current signals," *IEEE Trans. Ind. Electr.*, vol. 56, pp. 4710-4717, no. 11, Nov. 2009.

MCSA to detect generalized roughness

For these reasons, we have decided to diagnose the presence of generalized roughness by means of the analysis of both the current and the stray flux signals.

Previously, we have examined other bearing faults by means of the analysis of current and stray flux, but considering only the harmonics multiple of the fundamental.

L. Frosini, C. Harlişca, and L. Szabó, "Induction machine bearing faults detection by means of statistical processing of the stray flux measurements," *IEEE Trans. Ind. Electron.*, vol. 62, no. 3, March 2015.

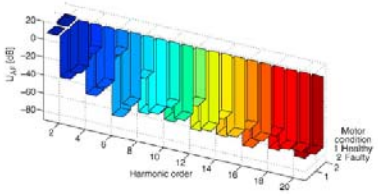

Fig. 4. Integer harmonics of the axial leakage flux.

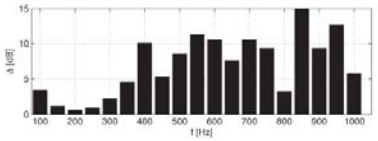

Fig. 5. Absolute value of the integer harmonics differences.

Then, we have decided to pay attention also to the characteristic components derived from the equations of the single-point bearing defects.

The test-bench

The bearing faults have been simulated on a three-phase induction motor, P_n = 2.2 kW, 2 poles, n_n = 2800 rpm, supplied by the mains (400 V, 50 Hz) and joined with a magnetic powder brake.

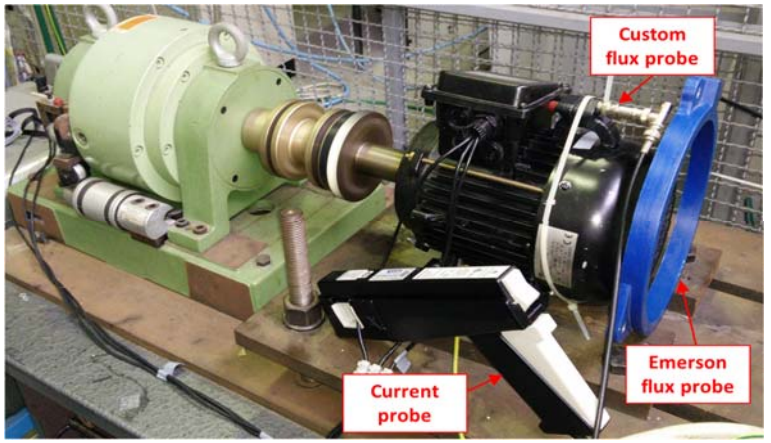

The test-bench

The ball bearings are double-crown, with a plastic cage which allows a simple disassembly of the balls. Generalized roughness was artificially created on all the balls of a bearing, at three progressive stages, by immersing the balls in a solution of concentrated sulfuric acid.

Therefore, four conditions of the bearing are available:

Healthy

Damage step 1

Damage step 2

Damage step 3

The experimental tests

The motor was tested in 8 different cases, at no-load and at 75% of the rated load, for each condition of the bearing.

In the faulty cases, the drive-end bearing of the motor was substituted with one of the artificially damaged bearings.

In order to obtain a robust diagnosis from a statistical point of view, for each case, a set of 40 acquisitions was collected: each acquisition consists of 2^{19} samples, gathered with a sampling frequency of 20 kHz.

In each acquisition, three variables have been measured in a synchronous way:

a) current of one phase;

b) axial leakage flux, by means of a commercial probe;

c) axial leakage flux, by means of a custom probe.

The experimental tests

- Each acquisition has been transformed in the frequency domain, in the range 0÷2000 Hz.
- The mean and the standard deviation of the 40 spectra related to each set of acquisitions have been calculated.
- The mean of the spectra related to each healthy case has been compared with the corresponding faulty cases.

The warning of possible fault is present when an excited harmonic appears within a range of ±5 Hz around each characteristic frequency of fault.

This "range of sensitivity" permits to overcome possible misunderstandings due to measurement errors or to small changes in the mechanical speed of the rotor, in order to make more robust the fault detection in industrial environment.

The experimental results

In the following tables, the characteristic frequencies of the single-point bearing faults are reported when the related harmonics reveal a difference in amplitude between the healthy and the faulty cases higher than three times the standard deviation of the healthy case.

Comparison	Variable	Characteristic harmonics [Hz]
GC3 vs. GC1 no-load, step 1	Current	640
	Emerson flux	**540**, 640
	Custom flux	**300**, **540**, 1400, 1500
GC4 vs. GC2 75% load, step 1	Current	930, **1030**
	Emerson flux	**30**, **300**, 400, 440, 520, **540**, 640, 930, **1030**, 1425, 1910
	Custom flux	**300**, 400, 440, 520, **540**, 930, **1030**, 1425, 1525

The experimental results

Comparison	Variable	Characteristic harmonics [Hz]
GC5 vs. GC1 no-load, step 2	Current	185
	Emerson flux	---
	Custom flux	185, **300**, **540**, 1400, 1500
GC6 vs. GC2 75% load, step 2	Current	---
	Emerson flux	**30**, 520
	Custom flux	**540**

Comparison	Variable	Characteristic harmonics [Hz]
GC7 vs. GC2 no-load, step 3	Current	70, 285, **300**
	Emerson flux	**30**, 70, 90, 170, 185, 285, **300**, 400, 420, 440, 520, **540**, 640, 670, 770, 930, **1030**, 1400, 1420, …
	Custom flux	5, **30**, 70, …, 170, 185, 285, **300**, 400, 420, 440, 520, **540**, 640, 670, 770, 930, **1030**, 1400, 1425, …
GC8 vs. GC2 75% load, step 3	Current	**300**, 520
	Emerson flux	**30**, 70, 105, …, 170, 190, 285, **300**, 400, 420, 440, 520, **540**, 640, 670, 770, 930, **1030**, 1400, 1425, …
	Custom flux	**30**, 185, 285, **300**, 400, 420, 440, 520, **540**, 640, 670, 770, 930, **1030**, 1400, 1425, 1500, 1520, 1910

The experimental results

Observations:

- the stray flux presents a more consistent diagnostic content with respect to the stator current, so its use as diagnostic indicator seems promising;
- the frequencies highlighted in bold are common to almost all the examined cases;
- the characteristic frequencies of the single-point bearing defects seem significant also in case of generalized roughness, provided to neglect the selectivity of the damaged component;
- the analysis of these frequencies has to be completed with the monitoring of the trend of all the harmonic spectrum;
- the detection ability of the custom flux probe seems more effective with respect to the commercial flux sensor.

The experimental results

Differences between the means of the spectra of the **custom flux** related to the cases GC1 and GC3 (no-load, **step 1**):

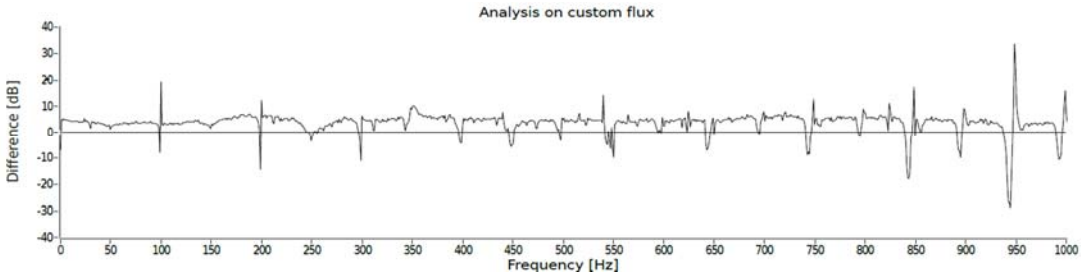

The experimental results

Differences between the means of the spectra of the **custom flux** related to the cases GC1 and GC5 (no-load, **step 2**):

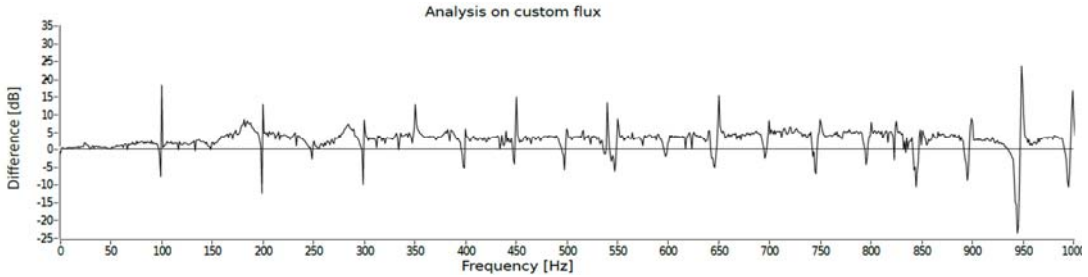

The experimental results

Differences between the means of the spectra of the **custom flux** related to the cases GC1 and GC7 (no-load, **step 3**):

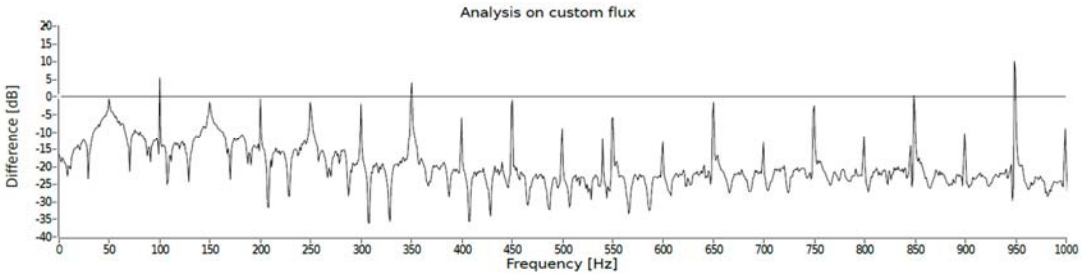

The experimental results

This method can be completed by a thermal analysis (the dimension of the red area increases with the damage degree):

Healthy

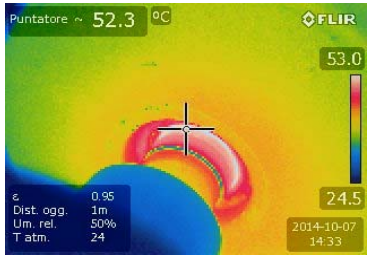

Damage step 1

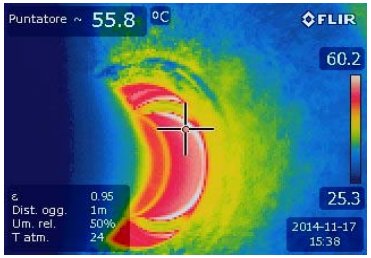

Damage step 2

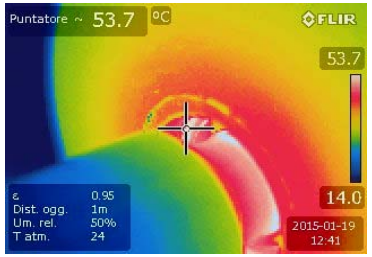

Damage step 3